hong Song for carrying out the photochemical reaction and James Chou for valuable assistance.

Registry No. **1b**, 46119-69-1; **1c**, 138337-13-0; **1d**, 100-88-9; **2b**, 138337-14-1; **2c**, 138337-15-2; **2d**, 138337-16-3; **3b**, 100-51-6; **3c**, 60-12-8; **3d**, 108-93-0; **4b**, 18687-57-5; **4c**, 138337-17-4; **4d**, 18687-60-0; **5b**, 3012-37-1; **6b**, 622-78-6; **7b**, 140-11-4; $PhCH_2NH_2$, 100-46-9; $ClSo_3H$, 7790-94-5; $Ph(CH_2)_2NH_2$, 64-04-0; NaSCN, 540-72-7; $PhCO_2H$, 65-85-0; AcOH, 64-19-7; $PhCO_2CH_2Ph$, 120-51-4; $PhCH_2OSO_3CH_2Ph$, 18495-74-4; $Ph(CH_2)_2OSO_3(CH_2)_2Ph$, 138337-18-5; PhCHO, 100-52-7; cyclohexylamine, 108-91-8; 1-phenylethylamine, 98-84-0; 1-phenylethyl alcohol, 98-85-1; cyclohexene, 110-83-8; ammonium benzylidenesulfamate, 22102-31-4; ammonium sulfamate, 7773-06-0; pepsin, 9001-75-6.

Synthesis of Multidentate Imidazole-Containing Macrocycles

Yung-Dong Choi and J. Paul Street*

Department of Chemistry, University of Houston, Houston, Texas 77204-5641

Received September 24, 1991

All three possible monomeric macrocyclic products and one dimeric product have now been isolated and spectrally characterized from the recently described[3] macrocyclization reaction which leads to imidazole-containing coronands. Alkali metal ion promoted reactions provide a small selectivity for the largest of the three monomeric macrocycles, coronand 1, and leads to improved yields (5–7%). Regioselective internal vs external N-alkylation of the imidazole derivatives of 1 is controlled by the counter cation employed. Small cations lead to external N-alkylation, while large cations lead to internal N-alkylation. This is evidence of selective cation binding within the cavity for the lithium and sodium imidazolates, but for potassium and larger ions, binding is at the external peripheral nitrogen atoms. Larger ions are likely excluded from the cavity because of the higher conformational energy costs involved. The X-ray structure of the symmetrically protected derivative of 1 has been obtained and confirms previous structural assignments.

Polydentate imidazole-containing ligands have found to be of general interest among bioinorganic research groups interested in metalloprotein model chemistry.[1] An active area of pursuit arising from such research is the synthesis of specially designed ligands with increasing degrees of conformational constraint.[2] Our own interests in this area prompted us to explore syntheses of imidazole-containing macrocycles, and in a recent communication[3] we reported the preparation and spectral characterization of the first member of a new imidazole coronand system, 1. In this paper we report improved experimental details and further coronand products that are obtained from this macrocyclization reaction. The X-ray crystal structure of the symmetrical 3,11,17,25-tetra-*N*-benzyl derivative of 1 has been determined and unambiguously confirms previous structural assignments.

Preparation of the Coronands. Coronand 1 is prepared from the reaction of *m*-xylylenediamine with 1,3-bis[1-benzyl-4-(2-(hydroxyimino)-1,3-dioxobutyl)-5-methylimidazol-2-yl]benzene, eq 1.[3] The macrocyclization reaction utilizes an imidazole condensation between benzylamines and oximes of β-dicarbonyl compounds.[4] Although yields in the final step are quite low, the synthetic route is both highly convergent and general, utilizing readily available starting materials. The precursor itself is prepared from *m*-xylylenediamine and 2-oximidopentanedione, and other (aminomethyl)heteroaromatics will also function in the imidazole-ring condensation.

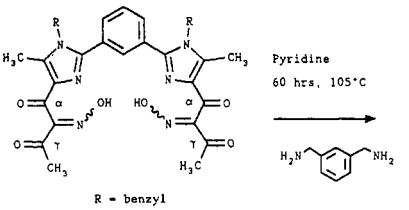

1, 3, 4, 5 (1)

Table I lists conditions of macrocyclization experiments in various solvents, in the presence of various metal ions, and in both batch and high dilution conditions. Dry pyridine has so far proved to be the best solvent. Although from the outset we have carried out these reactions using high-dilution techniques, equal yields have been obtained from simple batch reactions in cases without addition of metal salts (entries 5 and 10). By stepwise increases of reaction temperatures in batch experiments in pyridine, no reaction progress was observed to occur at temperatures up to 90 °C over a 24-h period. Aliquots of the reaction solution only showed unreacted starting materials (entry 9). Slow reaction progress begins to be observed at temperatures above 100 °C, and complete consumption of reactants occurs within 24 h at reflux temperatures. The near equivalence of both the high dilution and batch methods may be due to the slow reaction rate at 105 °C, the temperature used for most of the high-dilution experiments. The reaction in pyridine solvent eliminates the triimidazole side products, **2a** and **2b**, that were routinely isolated from reactions in sulfolane. Product **2a** and **2b**

(1) (a) Di Vaira, M.; Mani, F.; Stoppioni, P. *J. Chem. Soc., Chem. Commun.* **1989**, 127. (b) Knapp, S.; Keenan, T. P.; Zhang, X.; Fikar, R.; Potenza, J. A.; Schugar, H. J. *J. Am. Chem. Soc.* **1987**, *109*, 1882–1883. (c) Potvin, P. G.; Wong, M. H. *J. Chem. Soc., Chem. Commun.* **1987**, 672. (d) Buchanan, R. M.; Oberhausen, K. J.; Richardson, J. F. *Inorg. Chem.* **1988**, *27*, 971. Mashuta, M. S.; Webb. R. J.; Oberhausen, K. J.; Richardson, J. F.; Li, Q.; Hendrickson, D. N. *J. Am. Chem. Soc.* **1989**, *111*, 4497. Buchanan, R. M.; Mashuta, M. S.; Richardson, J. F.; Webb, R. J.; Oberhausen, K. J.; Nanny, M. A.; Hendrickson, D. N. *Inorg. Chem.* **1990**, *29*, 1299. (e) Brown, R. S.; Salmon, D.; Curtis, N. J.; Kusuma, S. *J. Am. Chem. soc.* **1982**, *104*, 3188. Brown, R. S.; Curtis, N. J.; Huguet, J. *J. Am. Chem. Soc.* **1981**, *103*, 6953. (f) Breslow, R.; Hunt, J. T.; Smiley, R.; Tarnowski, T. *J. Am. Chem. Soc.* **1983**, *105*, 5337.

(2) (a) Sorrell, T. N. *Tetrahedron* **1969**, *45*, 3–68. (b) Tolman, W. B.; Rardin, R. L.; Lippard, S. J. *J. Am. Chem. Soc.* **1989**, *111*, 4532 and references cited within. (c) van Veggel, F. C. J. M.; Bos, M.; Harkema, S.; van de Bovenkamp, H.; Verboom, W.; Reedijk, J.; Reinhoudt, D. N. *J. Org. Chem.* **1991**, *56*, 225 and references cited within. (d) Traylor, T. G.; Hill, K. W.; Tain, Z.-Q.; Reingold, A. L.; Peisach, J. McCracken, J. *J. Am. Chem. Soc.* **1988**, *110*, 5571–5573 and references cited within.

(3) Street, J. P. *Tetrahedron Lett.* **1991**, *32*, 3333.

(4) Veronese, A. C.; Cavicchioni, G.; Servadio, G.; Vecchiati G. *J. Heterocycl. Chem.* **1980**, *17*, 1723.

0022-3263/92/1957-1258$03.00/0

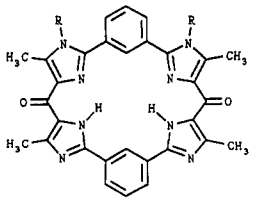

1 R = Benzyl

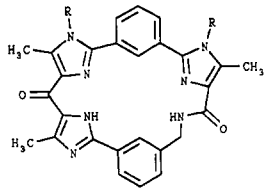

2a

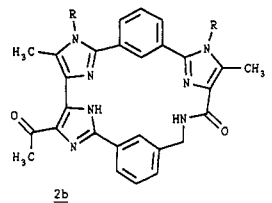

2b

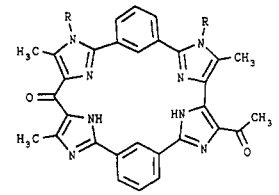

3

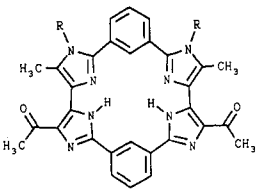

4

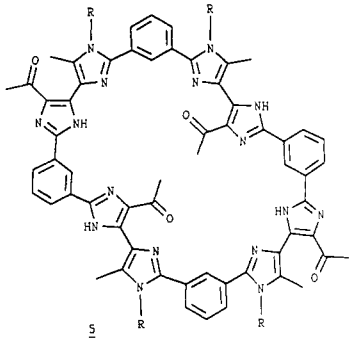

5

are thought to arise from a sulfolane-promoted Beckmann rearrangement of one of the oxime groups of the starting material, which subsequently leads to displacement and amide formation upon reaction with xylylenediamine.[5] These products are also noted in some of the alkali metal ion promoted reactions, which may be indicative of a Lewis acid role of the metal ion.

In the imidazole-ring condensation reaction there are two potential reaction paths, α or γ, defined by the carbonyl site which is initially attacked by the benzylamine (eq 1). All of the monomeric coronands expected from a combination of these two paths have now been isolated from the reaction in 1–2.5% yield (entry 5). Inclusion of alkali metal ions to the reaction medium provides modest enhancements in the yields of 1, consistently 5–6%, and at the same time yields of 3 and 4 are observed to decrease to ≤0.5%. The yield enhancement of 1 might be attributed to a combination metal ion template effect and Lewis acid catalysis. Best results have been obtained with calcium chloride; however, nearly equivalent results have been obtained using Li^+ and Mg^{2+}. Interestingly, univalent Li^+ and divalent Mg^{2+}, ions of similar size, provided equal enhancements. The metal ion effect has the appearance of a diversion of the reaction toward the γ-condensation path, resulting in 1 at the expense of 3 and 4. However, other α-condensation products (vide infra) are also obtained under these conditions, and the very small yields of monomeric products make such a conclusion very tenuous.

Under all of the reaction conditions mentioned above, we obtain a product which chromatographically elutes close to 3. The FAB-mass spectrum of this product gives a M + H^+ molecular ion peak with m/z = 1418, appropriate for a molecular dimer of 1, 3, or 4. By comparing the IR and ^{13}C-NMR spectra of this product with that of the monomeric coronands (Table II), and in consideration of its ^1H-NMR spectrum, we have tentatively assigned the structure of 5 (the $\alpha,\alpha,\alpha,\alpha$-condensation product). In particular, the ^{13}C-spectrum of 5 shows two distinct acetyl methyl resonances with accompanying carbonyl carbon signals as a result of the α-condensation path. The imidazole-ring methyl groups present in the starting material are seen as two signals and can be compared with those of coronand 4. No support for a γ-fused unit in the dimer can be found, such as a characteristic 1620 cm^{-1} carbonyl IR absorption or a ^{13}C signal at ≈15 ppm, which would be associated with a C-4 imidazole ring methyl group. The ^1H-NMR spectrum shows sets of signals for two benzyl groups, two central aryl groups, two imidazole N–H's, and four unique methyl groups. Each of the central arene groups is seen as a set of four equal-intensity signals with coupling connectivities confirmed by a COSY spectrum. The ^1H-NMR spectrum thus rules out any structure which has a C_2 axis running through the central arene groups, but is appropriate for a structure with an inversion center of symmetry without an accompanying C_2 axis or mirror plane. All aspects of the spectral data are best justified by the $\alpha,\alpha,\alpha,\alpha$-isomer, but with constraints from lying in its completely opened, maximum symmetry conformation. Structure 5 is one possibility (of several) which possesses the required symmetry. Molecular modeling shows the planar form of 5 to be free from any extreme angle strain.[6] The ring cavity size easily accommodates the inward rotation of two opposing substituted imidazole units, such as the indicated acetylimidazole moieties. This would alleviate steric interactions of ring substituents in the biimidazole units, thus providing the necessary conformer stabilization. It should be emphasized that other spectroscopically equivalent possibilities exist, such as an helical or saddle variation, for which 5 is merely the planar projection or the analogous structure with the 1-benzyl-5-methylimidazole moieties rotated inward. All of these conformers require consideration, and further conformational analysis and unambiguous structure proof will rest with obtaining a crystal structure. In these macrocyclization reactions the bulk of the mass balance is obtained as a precipitate of low solubility. We have generally ascribed this material to be a mixture of oligomeric condensation products. The isolation of a dimeric product 5 in addition to the monomeric structures generally supports this assessment.

Derivatives of Coronand 1. N-Protection of 1 provides an interesting example of chelate hole-size effects with this coronand. When the lithium or sodium salt of 1 is reacted with benzyl bromide in anhydrous DMF solution, the sole product obtained in high yield is **6a**, corresponding to alkylation of the outer peripheral imidazole nitrogen atoms.

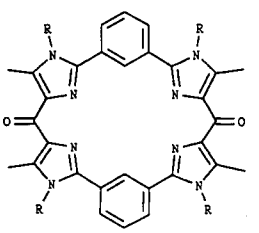

6a

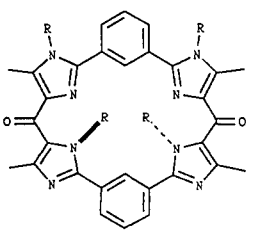

6b

(5) We have no ready answer for the sensitivity of the oxime compound in sulfolane. Decomposition is observed beginning at ≈80 °C; however the oxime is completely stable in refluxing DMF or pyridine. Perhaps trace acids remain in the sulfolane even after distillation from CaH_2 (see Experimental Section).

(6) Molecular mechanics calculations of the coronands were performed using PCModel by Serena Software, Bloomington, IN.

Table I. Macrocyclization Reaction Conditions and Yields

entry	solvent	condns[b]	add'n rate (mL/h)	total time (h)	temp (°C)	no. of runs	isolated yields[a] (%) 1	2a	2b	3	4	5
1	DMF	HD	0.24	44	140	6	1			U[c]	U	U
2	toluene	HD	0.24	44	118	1	1			U	U	U
3	MP[d]	HD	0.2	50	103	1	1.5			U	U	U
4	sulfolane	HD	0.2	50	136	8	2	0.5	0.5	U	U	U
5	pyridine	HD	0.2	67	105	6	2.5			1	1.5	0.5
6	pyridine	HD/LiCl	0.2	67	105	2	5			<0.5	<0.5	1.0
7	pyridine	HD/$MgBr_2$	0.2	68	105	2	5			<0.5	<0.5	1.0
8	pyridine	HD/$CaCl_2$	0.2	67	105	2	7			<0.5	<0.5	1.0
9	pyridine	batch		24	90	1	NR[e]			U	U	U
10	pyridine	batch		24	116	1	2.5			U	U	U
11	pyridine	batch/$CaCl_2$		24	116	1	3.5	0.5	0.5	U	U	U

[a] Yields are averages rounded to the nearest 0.5% from the number of experimental runs listed. [b] HD = high dilution conditions, see Experimental Section. Where added, 140 mM solutions of alkali metal salts were used. For the batch experiments, solutions 14 mM in reactants were employed, equivalent to the final proportions that would be obtained from high-dilution reactions. [c] Undetermined. [d] *N*-Methylpyrolidinone. [e] No reaction. Only starting reactants were found.

Table II. Comparison of Methyl and Carbonyl Group IR and ^{13}C-NMR Frequencies for Compounds 1–6

compd	IR (cm^{-1}) C=O	^{13}C-NMR (δ) C=O	CH_3
1	1624	176.2	11.1, 15.9
2a	1625, 1685	177.0, 163.6	9.63, 11.15, 16.34
2b	1678 (broad)	*a*	9.73, 11.01, 27.78
3	1620, 1680	176.9, 195.4	10.9, 11.6, 16.6, 27.9
4	1672	193.6	10.8, 27.4
5	1670	189.8, 194.9	9.1, 11.9, 28.2, 28.5
6a	1620	*a*	10.4
6b	1625	*a*	10.2, 14.2

[a] Due to limitations of sample, the signal was not observed after 12 h of aquisition time.

However, when K_2CO_3 or alkali bases with larger cations are used, the exclusive product is **6b**,[7] resulting from N-alkylation from within the interior of the macrocycle cavity. In the Cs_2CO_3 case, 70% yields of **6b** are obtained. We attribute this regioselectivity to metal ion directed alkylation at the uncomplexed nitrogen atom. In the small ion cases, internal ion chelation would direct alkylation to the periphery. However, potassium and larger ions apparently cannot fit the cavity without conformational deformation of the macrocycle and thus preferentially bind the outer peripheral nitrogen atoms resulting in interior alkylation. These results provide a qualitative measure of available space in the coronand cavity; selective for lithium and sodium, but binding larger ions in the interior only at a cost of higher conformational energy.[8] Obtaining product **6b** in high yields is a surprising result from the view point of steric accessibility of the coronand interior. The only energetically reasonable conformation obtained from molecular mechanics studies of **6b** has the two interior *N*-benzyl groups disposed anti to each other across the mean plane of the coronand.[6] The fact that this product is so readily obtained is indicative of the general nonrigidity of the coronand, which must have many energetically accessible puckering conformations.

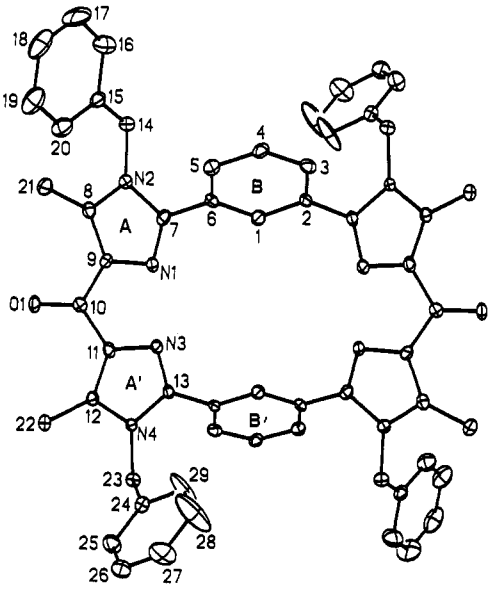

Figure 1. ORTEP structure of **6a** with hydrogen atoms omitted.

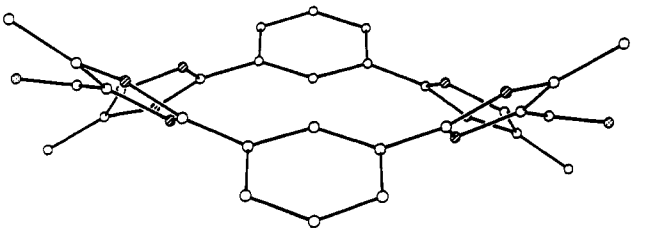

Figure 2. Side view of **6a** with the benzyl groups omitted.

X-ray Crystal Structure of 6a. Concentration of a $CDCl_3$ solution of **6a** gave single crystals as colorless plates. The crystals were sensitive to desolvation, and the packing structure was later found to contain the molecule lying parallel to the *ac* cell diagonal, separated by thick layers of solvent. The unit cell has a 6:1 $CDCl_3$/**6a** ratio. Each molecule of **6a** is situated on a local inversion center. Two peripheral *N*-benzyl groups of each ring are oriented roughly perpendicular to the mean plane of the macrocycle, and involved in Π stacking with like groups from adjacent molecules in the crystal cell. The ORTEP structure of the isolated coronand ring is given in Figure 1. The macrocycle core lies in a overall chair form with an approximate local C_2 axis running through the two carbonyl groups as shown in Figure 2. The least-squares planes of the two central arene rings (B, B′; Figure 1) define two parallel

(7) Clean reactions with complete consumption of starting material were obtained in every case by using excess benzyl bromide. With stoichiometric amounts of added benzyl bromide, appreciable amounts of starting material and tribenzyl products are obtained.

(8) Examination of computer-generated[6] CPK models of **6a** shows that little open interior space exists due to the presence of the hydrogen atoms of the central arene units projecting into the interior. Two metal ion binding loci exist at each diimidazole ketone unit. When all atoms of the macrocycle are constrained to lie in a plane, the space at each locus is found to accommodate a lithium ion, but sodium ion would begin to have repulsive contact with the interior hydrogens. Since the macrocycle is conformationally flexible however, larger ions could bind the "interior" at these loci by lying above the macrocycle mean plane in a chelate complex with N1 and N3 (Figure 1). Thus, the idea of a distinct "hole size" is somewhat artificial for this system.

Table III. Selected Torsion and Interplane Angles of 6a

	least-squares planes for internal 5- and 6-membered rings[a]			
torsion angles (deg)	mean deviation from planarity	(Å)	interplane dihedral angles	(deg)
O1–C10–C11–N3 147.5	A	0.005	AB	50.1
O1–C10–C11–C12 -31.1	B	0.163	AA′	49.6
N1–C9–C10–O1 155.9	A′	0.006	A′B′	54.6
C8–C9–C10–O1 -21.3	B′	0.119		
C8–N2–C14–C15 88.4				
C7–N2–C14–C15 -98.8				
C12–N4–C23–C24 -71.8				
C13–N4–C23–C24 93.6				

[a] Defined as in Figure 1.

planes offset by 2.26 Å. The internal 5- and 6-membered rings are essentially planar by least-squares, and the puckering dihedral angles associated with the eight free internal σ bonds of the macrocycle are in a range that is normal for simple substituted diaryl and diaryl ketone systems (Table III).[9] A complete listing of crystallographic data is provided in the supplementary material.

Conclusions

X-ray structural analysis of **6a** confirms the original structural assignment of **1** based on spectroscopy. Metal ion template and/or Lewis acid catalysis improves yields of the macrocyclization reactions and selects for coronand **1**. Further work will be required to achieve optimal yields; however, bearing in mind the ready availability of inexpensive precursors, useful amounts of **1** can now be obtained. Despite the low yields involved, we have been propelled by the uniqueness of **6a** and the potential for construction of conformationally constrained dinucleating ligands employing biologically relevant donors. In work to be described elsewhere, we have elaborated **6a** into a hexadentate ligand by the attachment of imidazole-bearing groups via the carbonyl centers. The resulting ligand is designed to be a close structural analogue of the known active site metal environment in dinuclear (type 3) copper proteins.[10] In addition, the reaction conditions can be controlled to allow the addition of only one pendant group, leading to an asymmetrical pentadentate ligand. The latter is of interest for the potential preparation of functional hemerythrin models.[11] Biomimetic studies of the metal ion complexes of these ligands and the associated redox chemistry is in progress.

Experimental Section

Pyridine, DMF, sulfolane, and *N*-methylpyrrolidinone were distilled from CaH_2 and stored under nitrogen. *m*-Xylylenediamine (Aldrich) was distilled in vacuo and stored under nitrogen. Benzyl bromide was distilled before use. Anhydrous magnesium bromide was prepared from magnesium and ethylene bromide in dry THF and collected and stored under nitrogen. All other metal salts were reagent grade and used as supplied. "Bakerflex" alumina, or silica analytical TLC plates were used. FAB mass spectra were obtained using *m*-nitrobenzyl alcohol matrix. *J* values are given in Hz in the NMR data.

General High-Dilution Macrocyclization Procedure. Separate solutions each 0.155 M of *m*-xylylenediamine and 1,3-bis[1-benzyl-5-methyl-4-(2-hydroxyimino)-1,3-dioxobutyl)-imidazol-2-yl]benzene[3] are prepared in degassed solvent. Aliquots (10 mL) of both solutions are synchronously added, at a rate of 0.2 mL/h by means of a dual syringe pump, to a stirred flask containing 100 mL of solvent under N_2 at the indicated temperatures (Table I). Heating is continued for at least 12 h beyond completion of addition. In cases where metal salts are employed, 16 mmol of the anhydrous salt is initially added to the reaction flask. The excess solvent is removed in vacuo, and the residue is taken up in a minimal amount of chloroform and then triturated with a 20× volume of ethyl acetate. A precipitate of oligomeric material is filtered away and washed with additional ethyl acetate. The combined filtrate is concentrated in vacuo, and the residue is chromatographed on alumina (activity grade III, 0–2% methanol/$CHCl_3$). Products are listed in order of elution.

Triimidazole Macrocycles 2a, 2b. From reactions performed in sulfolane utilizing 1.6 mmol reactants, 3 mg of **2a** is obtained (0.3%), R_f = 0.27 (alumina, 5:5:1 hexane/CH_2Cl_2/MeOH). FAB-MS: *m/z* 675 $(M + H_2O)^+$, 659 $(M + H_2)^+$ base peak. ^{1}H-NMR ($CDCl_3$): δ 2.51 (s, 3 H), 2.64 (s, 3 H), 2.77 (s, 3 H), 4.67 (d, 2 H, 4.2 Hz), 5.34 (s, 2 H), 5.37 (s, 2 H), 7.04 (broad s, 4 H), 7.24 (t, 1 H, 7.5 Hz), 7.27–7.4 (m, 8 H), 7.48 (t, 1 H, 7.8 Hz), 7.85 (s, 1 H), 8.09 (d, 2 H, 7.8 Hz), 8.31 (br t, 1 H, ≈4 Hz, NH), 8.66 (s, 1 H), 12.17 (br s, 1 H). ^{13}C-NMR ($CDCl_3$): δ 9.63, 11.15, 16.34, 43.15, 47.96, 48.31, 125.43, 125.50, 126.15, 126.90, 128.09, 128.18, 128.47, 128.67, 129.34, 129.45, 130.49, 131.33, 131.92, 132.92, 133.01, 135.57, 135.84, 136.28, 138.62, 138.94, 145.25, 146.44, 147.36, 163.60, 176.98. IR (cm^{-1}) 3400, 1685, 1625, 1570, 1528.

2b (2.5 mg) is obtained (0.2%), R_f = 0.24 (alumina, 5:5:1 hexane/CH_2Cl_2/MeOH). FAB-MS: *m/z* 675 $(M + H_2O)^+$, 659 $(M + H_2)^+$ base peak, 568 $(M - C_7H_5)^+$. ^{1}H-NMR ($CDCl_3$): δ 2.51 (s, 3 H), 2.55 (s, 3 H), 2.74 (s, 3 H), 4.78 (d, 2 H, 4.5 Hz), 5.39 (s, 2 H), 5.41 (s, 2 H), 7.05 (d, 2 H, 7.2 Hz), 7.13, (d, 2 H, 7.5 Hz), 7.18 (d of d, 1 H), 7.23–7.41 (m, 9 H), 7.48 (t, 1 H, 7.5 Hz), 8.03 (s, 1 H), 8.07 (d, 7.5 Hz), 9.26 (s, 1 H), 11.68 (s, 1 H). ^{13}C-NMR ($CDCl_3$, upfield region): δ 9.73, 11.01, 27.78, 41.88, 48.04, 48.20. IR (cm^{-1}): 3400, 1678, 1598, 1525.

26-Acetyl-3,11-dibenzyl-2,12,16-trimethyl-3,11,17,25,28,-30,31,33-octaazaheptacyclo[23.2.1.1^{5,9}.1^{10,13}.1^{15,18}.1^{19,23}.1^{24,27}]-tritriaconta-1,4(28),5(29),6,8,10(30),12,15,17,19,21,23-(32),24,26-tetradecaen-14-one (3). After passing high R_f impurities and remaining solvent, **1**[3] elutes (R_f = 0.53; analytical alumina TLC, 2% methanol/$CHCl_3$), followed closely by **3**. Coronand **3** is purified further by successive TLC on silica using 5% methanol/$CHCl_3$ (R_f = 0.38). FAB-MS: *m/z* 709 $(M + H^+)$. ^{1}H-NMR ($CDCl_3$) δ 2.59 (s, 3 H), 2.60 (s, 3 H), 2.73 (s, 3 H), 2.77 (s, 3 H), 5.35 (s, 2 H), 5.42 (s, 2 H), 7.03 (d, 2 H), 7.12 (d, 2 H), 7.2–7.4 (m, 7 H), 7.61 (t, 1 H, 7.5 Hz), 8.12 (d, 1 H, 7.5 Hz), 8.13 (s, 1 H), 8.35 (d, 1 H, 8.1 Hz), 8.78 (s, 1 H), 11.69 (s, 1 H), 11.88 (s, 1 H). ^{13}C-NMR ($CDCl_3$, 33 of 40 signals were observed): δ 10.96, 11.61, 16.59, 27.85, 48.27, 48.56, 121.0 (broad), 125.17, 125.37, 125.47, 125.73, 125.83, 127.63, 127.79, 127.86, 127.99, 128.05, 128.58, 129.03, 129.20, 129.33, 129.46, 130.14, 130.24, 130.33, 131.19, 131.68, 135.52, 135.64, 145.59, 145.72, 176.98, 195.4. IR (cm^{-1}): 1680, 1620, 1565. UV (95% ethanol): λ 278, 310 (shoulder). Anal. Calcd for $C_{44}H_{36}N_8O_2$: C, 74.55; H, 5.12. Found: C, 74.51; H, 5.20.

15,25-Diacetyl-3,11-dibenzyl-2,12-dimethyl-3,11,16,24,27,-29,30,32-octaazaheptacyclo[22.2.1.1^{5,9}.1^{10,13}.1^{14,17}.1^{18,22}.1^{23,26}]-dotriaconta-1,4(27),5(28),6,8,10(29),12,14,16,18,20,22-(31),23,25-tetradecaene (4). Products **4** and **5** coelute in a single fraction from the alumina column. On standing, **4** crystallizes from this mixture after partial evaporation. FAB-MS: *m/z* 709 $(M + H^+)$. ^{1}H-NMR (DMSO-d_6/TMS): δ 2.34 (s, 6 H), 2.59 (s, 6 H), 5.61 (s, 4 H), 7.07 (d, 4 H), 7.24–7.37 (m, 7 H), 7.55 (d, 7.2 Hz, 2 H), 7.66 (t, 7.5 Hz, 1 H), 7.91 (d, 7.5 Hz, 2 H), 8.39 (s, 1 H), 9.82 (s, 1 H), 12.78 (s, 2 H). ^{13}C-NMR (DMSO-d_6): δ 10.78, 27.39, 47.27, 124.00, 124.33, 125.34, 125.58, 125.82, 127.45, 128.21, 128.59, 128.89, 129.63, 130.32, 130.51, 130.82, 131.64, 135.63, 136.73, 144.32, 145.40, 193.55. IR (KBr) (cm^{-1}): 3400 (br), 1672 (s), 1510 (m), 1409 (s), 1355. Anal. Calcd for $C_{44}H_{36}N_8O_2$: C, 74.55; H, 5.12. Found: C, 74.34, H, 5.18.

Dimeric Product 5. The fraction containing **5** is purified of remaining **4** by successive TLC on silica (10% methanol/CH_2Cl_2). FAB-MS: *m/z* 1417.9 (exact mass $C_{88}H_{72}N_{16}O_4 + H^+$, 1417.6). ^{1}H-NMR ($CDCl_3$): δ 1.82 (s, 6 H), 1.83 (s, 6 H), 2.58 (s, 6 H), 2.80 (s, 6 H), 4.83 (s, 4 H), 5.01 (s, 4 H), 6.21 (d, 2 H, 7.8 Hz), 6.55 (t, 2 H, 7.8 Hz), 6.69 (d, 4 H, 7.2 Hz), 6.89 (d of d, 4 H, 7.5, 3.6 Hz),

(9) (a) *Structure Reports*; Pearson, W. B., Ferguson, G., Eds.; Oosthoek, Scheltema, & Holkema: Utrecht, 1967; Vol. 32B. (b) *Crystal Structures*; Wyckoff, R. W. G., Ed.; Wiley Interscience: New York, 1971; Vol. 6.

(10) Tyeklar, Z.; Karlin, K. D. *Acc. Chem. Res.* **1989**, *22*, 241.

(11) Lippard, S. J. *Angew. Chem., Int. Ed. Engl.* **1988**, *27*, 344.

6.97 (d, 2 H, 7.8 Hz), 7.06-7.16 (m, 8 H), 7.29 (t, 4 H), 7.36 (t, 2 H, 7.8 Hz), 7.56 (d, 2 H, 7.8 Hz), 7.57 (s, 2 H), 8.27 (d, 2 H, 7.8 Hz), 9.15 (s, 2 H), 11.47 (s, 2 H, imidazole N-H), 14.27 (s, 2 H, imidazole N-H). ^{13}C-NMR ($CDCl_3$, 31 of 40 expected signals were observed): δ 9.10, 11.98, 28.24, 28.51, 48.20, 48.94, 125.45, 125.53, 126.48, 127.33, 127.58, 127.70, 128.22, 128.51, 129.04, 129.42, 129.57, 129.78, 129.90, 130.55, 131.57, 132.75, 136.08, 136.51, 137.11, 142.35, 145.35, 146.62, 148.32, 189.75, 194.87. IR (cm^{-1}): 2950, 1680 (s), 1560 (w), 1465 (m). Anal. Calcd for $C_{88}H_{72}N_{16}O_4$: C, 74.55; H, 5.12. Found: C, 74.61; H, 5.12.

LiOH- and NaOH-Promoted N-Benzylation of 1 and 6a. 1 (5 mg, 7.05 μmol) is placed in a 5-mL flask with 1 mg of LiOH or NaOH and a spatula tip full of powdered 4A molecular sieves. A 150-μL portion of a 0.116 M benzyl bromide solution in DMF is added and the mixture stirred 1 h at room temperature. The temperature is then raised to 75 °C for 17 h. The mixture is diluted with $CHCl_3$ and filtered, and volatiles are removed in vacuo. TLC chromatography (alumina, 50:50 v/v $CHCl_3$, EtOAc; R_f = 0.16) provides 5.5 mg (88%) of **6a**, which crystallizes from $CHCl_3$/EtOAc as a white powder, mp > 310 °C. FAB-MS: m/z 889.6 (exact mass $C_{58}H_{48}N_8O_2 + H^+$ = 889.4). ^{1}H-NMR ($CDCl_3$): δ 2.59 (s, 12 H), 5.24 (s, 8 H), 7.08 (t, 2 H), 7.14 (d, 8 H, 7.21 Hz), 7.19 (d, 4 H), 7.33 (t, 4 H), 7.38 (d of d, 8 H), 8.93 (s, 2 H). ^{13}C-NMR ($CDCl_3$, the carbonyl signal was not observed): δ 10.36, 48.27, 125.77, 127.26, 127.34, 127.54, 127.83, 129.26, 131.48, 132.747, 136.16, 136.37, 146.44. IR (cm^{-1}): 1620, 1560, 1405, 880.

K_2CO_3-, Rb_2CO_3-, and Cs_2CO_3-Promoted N-Benzylation of 1 and 6b. 1 (3.4 mg, 4.8 μmol) is placed with 4 mg of cesium carbonate in a 5-mL flask, and 100 μL of a 0.116 M DMF solution of benzyl bromide is added. After stirring at room temperature for 1 h, the temperature is raised to 75 °C for 21 h. TLC chromatography (alumina, 20:20:1 v/v $CHCl_3$/EtOAc/EtOH; R_f = 0.16) gave 3.0 mg (70%) of **6b** as a solid residue. FAB-MS: m/z 889.6 ^{1}H-NMR ($CDCl_3$): δ 2.30 (s, 6 H), 2.54 (s, 6 H), 5.27 (s, 4 H), 5.67, 5.96 (AB quartet, 4 H), 6.50 (d, 4 H, 7.2 Hz), 6.98 (d of d, 4 H), 7.06 (d, 4 H, 6.3 Hz), 7.1-7.4 (m, 11 H), 7.65 (t, 1 H, 7.5 Hz), 7.99 (d, 2 H, 7.5 Hz), 8.06 (s, 1 H), 8.34 (s, 1 H). ^{13}C-NMR ($CDCl_3$) upfield region: δ 10.53, 14.55, 48.08, 52.17. IR (cm^{-1}): 1625, 1555, 890. Analogous reactions, employing excesses of either rubidium carbonate or potassium carbonate were performed as above. The reaction mixture was analyzed by TLC by comparison with authentic samples, showing **6b** as the sole product.

Acknowledgment. We are grateful to the Robert A. Welch Foundation for support of this work. We thank Prof. Royal Freas for assistance with FAB-MS, James Korp for the crystal structure determination, and Pierre Hartmann for preparations of starting materials.

Registry No. 1, 137389-54-9; **2a**, 138286-12-1; **2b**, 138286-13-2; **3**, 138286-14-3; **4**, 138286-15-4; **5**, 138286-16-5; **6a**, 138286-17-6; **6b**, 138286-18-7; *m*-xylylenediamine, 1477-55-0; 1,3-bis[1-benzyl-5-methyl-4-(2-(hydroxyimino)-1,3-dioxobutyl)imidazol-2-yl]benzene, 137389-52-7.

Supplementary Material Available: Complete crystal structure parameters for **6a**, including atomic positional and thermal parameters; ^{1}H-NMR and FAB-MS for compounds **2-6** (20 pages). Ordering information is given on any current masthead page.

5,6,11,12-Tetrahydrochrysenes: Synthesis of Rigid Stilbene Systems Designed To Be Fluorescent Ligands for the Estrogen Receptor

Kwang-Jin Hwang, James P. O'Neil, and John A. Katzenellenbogen*

Department of Chemistry, University of Illinois, 1209 West California Street, Urbana, Illinois 61801

Received July 2, 1991 (Revised Manuscript Received October 22, 1991)

We have prepared a series of tetrahydrochrysenes as fluorescent ligands for the estrogen receptor. The stilbene chromophore in this tetracyclic system is held rigid and is adorned with an electron-donating hydroxyl group at C-8 that corresponds to the phenolic hydroxyl of estrogens and an electron acceptor at C-2 to give a donor-acceptor fluorophore. Additional substituents at C-5 and C-11 provide additional bulk that improves receptor binding affinity without distorting the planar conjugated system. The tetrahydrochrysene core was prepared by an acyloin condensation of α-alkyl *m*-methoxyhydrocinnamate esters, followed by a double dehydrative cyclization. The cis and trans isomers of the alkyl substituted systems could be separated and their stereochemistry ascertained by X-ray crystallographic analysis; the trans isomer has the higher receptor binding affinity, and the derivative with ethyl substituents at C-5 and C-11 has the best affinity. The donor-acceptor systems were prepared by functional group manipulations on one of the aromatic methoxy groups: conversion to the trifluoromethanesulfonate was followed by a palladium-mediated carbonylation to give the acetyl derivative and methoxycarbonylation to give the ester. The ester was further elaborated to the amide and nitrile. The nitro compound was prepared by nitration of protio system, itself prepared by hydrogenolysis of the trifluoromethanesulfonate. As will be described later, these tetrahydrochrysenes provide a favorable combination of estrogen receptor binding affinity and long wavelength, high quantum yield fluorescence to make them useful as fluorescent ligands for the estrogen receptor.

Introduction

Fluorescent probes have proved to be widely useful in characterizing cellular binding sites, providing both quantitation and spacial resolution.[1] In this regard, there has been a longstanding interest in the development of fluorescence-based methods for detecting steroid receptors that might permit a cell-by-cell assay of receptor content in hormone responsive cells.[2-5] Of particular interest is

(1) (a) Lakowicz, J. R. *Principles of Fluorescence and Spectroscopy*; Plenum: New York, 1983 and references cited therein. (b) Taylor, O. L.; Waggoner, A. S.; Murphy, R. F.; Lanni, F.; Birge, R. R. *Applications of Fluorescence in the Biomedical Science*; Alan R. Liss: New York, 1985.

(2) For immunofluorescence methods, see: (a) Mercer, W. D.; Edward, D. P.; Chamness, G. C.; McGuire, W. L. *Cancer Res.* **1981**, 4644. (b) Stumpe, W. E.; Sar, M. *Acta Histochem. Cytochem.* **1982**, 560. (c) Pertschuk, L. P.; Tobin, E. H.; Carter, A. C.; Eisenberg, K. B.; Leo, V. C.; Gaetjens, E.; Bloom, N. D. *Breast Cancer Res. Treat.* **1981**, 297 (1) and references cited therein.

0022-3263/92/1957-1262$03.00/0